Genes, Brain and Behavior (2008) **7:** 78–87

Strain- and region-specific gene expression profiles in mouse brain in response to chronic nicotine treatment

J. Wang[†], R. Gutala[†], Y. Y. Hwang[†], J.-M. Kim[†], O. Konu[‡], J. Z. Ma[§] and M. D. Li*[,†]

[†]Department of Psychiatry and Neurobehavioral Sciences, University of Virginia, Charlottesville, VA, USA, [‡]Department of Genetics and Molecular Biology, Bilkent University, Ankara, Turkey, and [§]Department of Public Health Sciences, University of Virginia, Charlottesville, VA, USA

**Corresponding author: Ming D. Li, PhD, Section of Neurobiology, University of Virginia, 1670 Discovery Drive, Suite 110, Charlottesville, VA 22911, USA. E-mail: ml2km@virginia.edu*

A pathway-focused complementary DNA microarray and gene ontology analysis were used to investigate gene expression profiles in the amygdala, hippocampus, nucleus accumbens, prefrontal cortex (PFC) and ventral tegmental area of C3H/HeJ and C57BL/6J mice receiving nicotine in drinking water (100 μg/ml in 2% saccharin for 2 weeks). A balanced experimental design and rigorous statistical analysis have led to the identification of 3.5–22.1% and 4.1–14.3% of the 638 sequence-verified genes as significantly modulated in the aforementioned brain regions of the C3H/HeJ and C57BL/6J strains, respectively. Comparisons of differential expression among brain tissues showed that only a small number of genes were altered in multiple brain regions, suggesting presence of a brain region-specific transcriptional response to nicotine. Subsequent principal component analysis and Expression Analysis Systematic Explorer analysis showed significant enrichment of biological processes both in C3H/HeJ and C57BL/6J mice, i.e. cell cycle/proliferation, organogenesis and transmission of nerve impulse. Finally, we verified the observed changes in expression using real-time reverse transcriptase polymerase chain reaction for six representative genes in the PFC region, providing an independent replication of our microarray results. Together, this report represents the first comprehensive gene expression profiling investigation of the changes caused by nicotine in brain tissues of the two mouse strains known to exhibit differential behavioral and physiological responses to nicotine.

Keywords: Brain regions, C57BL/6J mice, C3H/HeJ mice, microarray, nicotine, PCA

Received 22 December 2006, revised 8 April 2007, accepted for publication 10 April 2007

Nicotine is the primary component in tobacco that maintains habitual smoking by affecting various molecular and cellular processes throughout the central nervous system (CNS) (Wonnacott *et al.* 2005). By acting on a diverse set of nicotinic acetylcholine receptors (nAChRs) within the CNS, nicotine directly or indirectly modulates the signaling pathways of a target neuron. Animal studies have indicated that nicotine, like other drugs of abuse, stimulates dopamine secretion in the outer shell of the nucleus accumbens (NA) (Pontieri *et al.* 1996; Robbins & Everitt 1999). Moreover, nicotine increases the extracellular levels of the excitatory amino acids, glutamine and aspartic acid in the ventral tegmental area (VTA) through stimulation of nAChRs (Schilstrom *et al.* 2000). Involvement of nicotine in both dopaminergic and glutamergic neurotransmission also may contribute to its addictive potential and relation to neuropsychiatric disorders such as Alzheimer's disease, Parkinsonism and schizophrenia (Mihailescu & Drucker-Colin 2000).

Behavioral and pharmacologic studies indicate that C3H/HeJ and C57BL/6 mice differ markedly in a number of nicotine-related behaviors [for a review, see Crawley *et al.* (1997)]. For example, C3H/HeJ mice develop tolerance only at high doses of chronically infused nicotine, whereas C57BL/6 animals do at much lower doses (Marks *et al.* 1991). A low dose of nicotine increases the locomotor activity in C3H/HeJ mice but depresses it in C57BL/6 mice (Marks *et al.* 1983). C57BL/6 mice also consume significantly more nicotine than do C3H/HeJ animals (Robinson *et al.* 1996). Moreover, mice of the two strains differ in their clearance of nicotine and its metabolites such as cotinine and nicotine *N*-oxide (Petersen *et al.* 1984). For example, the half-life of nicotine *N*-oxide in liver is greater in C57BL/6 than C3H/HeJ mice. Given such obvious behavioral and pharmacological differences in the response to chronic nicotine treatment between the two strains, it would be interesting to determine which gene(s) and biochemical pathway(s) are associated with these behavioral characteristics.

Previous studies have shown that nicotine modulates the expression of various genes in the CNS, including those involved in catecholamine and neuropeptide synthesis and transcriptional activation (Harlan & Garcia 1998; Li *et al.* 2000; Pich *et al.* 1997). Recently, using focused complementary DNA (cDNA) microarrays, we determined that the transcriptional response to nicotine administration in rats was brain-region and time dependent (Konu *et al.* 2001; Li *et al.* 2004). Furthermore, we identified several functional groups of genes both *in vivo* and *in vitro* as likely targets of nicotine addiction, such as those belonging to the phosphatidylinositol (PI) and growth factor-signaling pathways and the ubiquitin family (Konu *et al.* 2001, 2004; Li *et al.* 2002, 2004). The primary purpose of the present study was to identify and characterize

doi: 10.1111/j.1601-183X.2007.00328.x

the gene expression profiles in the amygdala, hippocampus, NA, prefrontal cortex (PFC), and VTA of the C3H/HeJ and C57BL/6J mouse strains in response to chronic oral nicotine administration using a pathway-focused cDNA microarray developed recently in this laboratory.

Materials and methods

Animals and brain tissue collection

Two-month-old male C3H/HeJ and C56BL/6J mice purchased from the Jackson Laboratory (Bar Harbor, ME, USA) were housed in wire-bottom cages in the 12/12 h light/dark cycle and were allowed food and water *ad libitum*. Animal received either nicotine tartrate (pH 7.0; Sigma, St Louis, MO, USA) through their drinking water at a dose of 100 μg/ml as free base in 2% saccharin solution (treatment group) or 2% saccharin alone (control group) for 14 days (Sparks & Pauly 1999). All experimental protocols were approved by the Institutional Animal Use Committee. Ten animals from each strain (five for the control and five for the nicotine-treated group) were included in the microarray and the quantitative RT–PCR verification experiments, separately.

After 2 weeks of nicotine treatment, mice were killed with a lethal overdose of sodium pentobarbital, and the brains were dissected out immediately after decapitation. After 2-mm brain slices were cut using a Stoelting tissue slicer (Stoelting, Chicago, IL, USA), bilateral punches were excised from the amygdala, anterior area of the hippocampus, NA, PFC and VTA using a bilateral 2.0-mm-diameter brain punch tissue set (myNeuroLab.com, St Louis, MO, USA) according to the co-ordinates of Paxinos & Franklin (2001) in a dish containing ice-cold saline. All the tissues were stored at −80°C until RNA isolation.

RNA isolation and reverse transcription, cDNA probe labeling, hybridization and image analysis

Total RNA was isolated separately from each brain region of each mouse using Trizol reagent (Invitrogen, Carlsbad, CA, USA) and was amplified as described previously for adequate cDNA probe labeling (Gutala *et al.* 2004; Konu *et al.* 2004). The detailed procedures for cDNA probe labeling and hybridization were the same as reported previously (Gutala *et al.* 2004; Li *et al.* 2004). Briefly, 2 μg of amplified RNA was added to a cocktail consisting of 4 μl of 5× RT buffer, 2 μl of 0.1 M dithiothreitol (DTT), 5 μl of 10 mM dNTPs mixture, 1 μl of RNasin, 4 μg of Cy3-labeled random nanomer (Tri-Link Technology, San Diego, CA, USA) and 2 μl of Superscript II reverse transcriptase (Invitrogen). The RT reaction was carried out at 42°C for 1.5 h, and the mixture was incubated at 85°C for 5 min to inactivate the enzyme. The purified cDNA probes were mixed with hybridization solution consisting of 25% formamide, 3× saline sodium citrate (SSC) and 0.1% sodium dodecyl sulphate (SDS). A homeostatic pathway-focused microarray consisting of 638 sequence-verified genes was used (Konu *et al.* 2004). The slides were hybridized for approximately 16 h at 42°C and washed in 1× SSC and 0.1% SDS at 42°C for 10 min followed by washing in 0.1× SSC, 0.2% SDS and 0.1× SSC for 5 min each at room temperature. Scanning was performed using the GenePix 4000B scanner and the intensities were quantified with GenePix 4.1 software (Axon Instruments, Union City, CA, USA).

Data normalization and statistical analysis

For each slide, the logarithmically transformed (on base 2) background-subtracted median intensity was used for further analysis. As in previous studies, the two replicates of each probe on the microarrays were treated as independent measurements (Konu *et al.* 2004; Li *et al.* 2004). The duplicate spots pairs with relative large intensity difference as indicated by an iteratively reweighted least-square algorithm (robustfit function; Matlab™; The Mathworks, Natick, MA, USA) were considered unreliable and excluded from further analysis (Konu *et al.* 2004). Data from each brain region of either strain were normalized using a *cyclic lowess* (locally weighted linear regression) to make replicates/slides comparable (Edwards 2003). In this procedure, a subset of normalization probes that appeared to be least regulated across each replicate pair were identified to construct a normalizing curve with parameters, $P = 0.015$ and $l = 15$. Normalized measurements of each gene within an experimental group were subjected to an outlier-detection procedure (Li *et al.* 2004) such that a gene was removed from further analysis if there were fewer than six valid measurements in either the control or the nicotine treatment group after removal of the outliers. Furthermore, the normalized data of only those genes with fold changes <0.85 or >1.15 between the nicotine-treated and control samples for each region were subjected to Student's *t*-test to detect the genes significantly regulated by nicotine ($P < 0.05$).

Principal component analysis (PCA) is a multivariate statistical method used to exploit essential factors to define a pattern in a data set by reducing the effective dimensionality of the data set (Crescenzi & Giuliani 2001). Specifically, PCA was implemented in the following way in this study: for each mouse strain, the normalized measurements were extracted for all the five brain regions for the genes differentially expressed in one or more regions. To reduce variation among the data of control samples, for each brain region, we averaged the normalized expression of controls for each gene and subtracted the mean from the normalized expression values of the nicotine-treated group. Then, the adjusted data from the five brain regions were merged and subjected to PCA with genes as variables and measurements as observations. The PCA analysis was performed using Matlab™.

Categorization of biological process using Gene Ontology

Procedure of Expression Analysis Systematic Explorer (EASE) (Hosack *et al.* 2003) was used to assign the significantly differentially expressed genes to ''GO: Biological Process'' categories of the Gene Ontology Consortium (www.geneontology.org). For genes whose biological process categories were not available in the EASE data sets, SOURCE (http://source.stanford.edu) also was searched to retrieve the relevant information. The categories with very few genes were merged with related categories. EASE analysis was carried out to test significance of enrichment for the co-expressed gene sets within each biological process category; an EASE score of 0.15 or less was considered significant (Blalock *et al.* 2004).

Validation of microarray results by quantitative real-time RT–PCR

The microarray results for six representative genes were validated using quantitative real-time RT–PCR (qRT–PCR) on RNA samples extracted from an independent animal experiment as previously described (Gutala *et al.* 2004; Konu *et al.* 2004). Briefly, PCR was carried out in 25 μl containing 1 μl of 12.5 mM dNTPs, 1× PCR buffer and 2.5 U of *Taq*Man or SYBER green on the ABI 7000 sequence detection system (Applied Biosystems, Foster City, CA, USA). A duplicate was run for each sample, along with a no-template control. 18 S ribosomal RNA was used as an internal control to normalize the expression levels of a target gene. The qRT–PCR data were analyzed using a comparative C_t method (Winer *et al.* 1999). Primer sequences were selected according to the cDNA sequence printed on the microarray for Homer homolog 2 (*homer2*): 5′-AGGGCAGGGATGTT-TAGATCTTC-3′ (forward) and 5′-CCCCATCCCCGGTTCATA-3′ (reverse) and amyloid beta A4 precursor protein binding, family B, member 2 (*Apbb2*): 5′- TCGGCCACATCGCATTCT-3′ (forward) and 5′- GGTATGCAGGCGATCTTTGTTC-3′ (reverse). For the other four genes, amyloid beta (A4) precursor protein (*App*), amyloid beta (A4) precursor-like protein 2 (*Aplp2*), inhibitor of kappa light polypeptide gene enhancer in B cells, kinase epsilon (*Ikbke*) and glutamate receptor, ionotropic, alpha-amino-3-hydroxy-5-methyl-4-isoxaolpropionate (AMPA 2)

(*Gria2*), the primers and *Taq*Man probes were purchased from ABI, and no sequence information was provided by the vendor.

Results

Identification of genes regulated by chronic nicotine treatment

The microarray analysis results may include a large number of false positives arising from multiple comparisons. To identify significantly regulated genes while minimizing multiple comparison error, one may choose to use a more stringent *P* value in identification of differentially expressed genes with the tradeoff of producing more false negatives. Another way is to filter the microarray data in reducing the number of tests need to be performed because for a given *P* value, the number of expected false positives is proportional to the total number of comparisons (Blalock *et al.* 2004, 2005).

Previous work from this and other laboratories has indicated that the changes in expression level of modulated genes by nicotine were subtle both *in vivo* and *in vitro* (Dunckley & Lukas, 2003; Konu *et al.* 2001, 2004; Li *et al.* 2004); thus might present potential problems in the downstream validation experiments. Given these considerations, use of a fold difference of 15% between the treatment and control groups as a cutting point helped keep a balance between the number of significantly regulated genes identified and the false discovery rate (FDR) for all the brain regions of the two strains. In our case, the expected false positives was calculated as the product of the number of genes tested and *P*, while the total number of positives was the number of genes with fold change difference $\geq$15% and $P < 0.05$. By doing so, we greatly reduced the number of genes to be tested for each brain region of both strains. For C3H/HeJ, 44, 40, 102, 288 and 198 genes and for C57BL/6J, 164, 86, 219, 55 and 34 genes were kept for statistical testing for amygdala, hippocampus, NA, PFC and VTA, respectively.

The number of differentially expressed genes varied greatly among the five brain regions of either strain (Tables 1, S1 and S2). For example, nicotine treatment of the C3H/HeJ mouse resulted in 22, 32, 94, 111 and 141 differentially expressed genes in the amygdala, hippocampus, NA, PFC and VTA, respectively, representing 3.5–22.1% of the 638 genes, and the FDRs were in the range of 0.05–0.13. There were also more upregulated genes than downregulated in four of the five regions with the exception being the hippocampus. However, in the C57BL/6J mice, differentially expressed gene numbers were 46, 46, 91, 30 and 24 in the amygdala, hippocampus, NA, PFC and VTA, respectively (Table 1), representing 4.1–14.3% of the 638 genes with FDRs ranging from 0.09 to 0.18. In this case, more downregulated than upregulated genes in the VTA of C57BL/6J mice were observed.

For the C3H/HeJ strain, a total of 312 genes were significantly modulated in the presence of nicotine in at least one brain region, and of these 77 were modulated in two or more regions. However, only seven of them (i.e. *Adrald*, *Avp*, *Loc245960*, *Pbx3*, *Pcp4*, *Pla2g4a* and *Pou5f1*; Table S3) were differentially modulated in three regions. For the C57BL/6J strain, expressions of 190 genes were changed significantly in at least one brain region, and 28 of them were modulated in at least two regions. However, only 4 of these 28 (i.e. *Gria2*, *Gtse1*, *Nr1d1* and *Slc6a4*; Table S4) were common in three or more regions.

Table 2 lists the genes significantly regulated in each brain region of both mouse strains. In the amygdala, *Usp2*, *Il15*, *Gsk3b* and *Kcr1* messenger RNA (mRNA) expression showed a striking inverse direction in their modulation by nicotine between the two strains, while *Pcp4*, *Psmb2*, *Rpl30* and *Tcfeb* in the hippocampus were modulated in the same direction. Among the 18 co-expressed genes in the NA, most were upregulated in both strains except that *Hap1*, *Celsr3*, *Rock1*, *Accn1*, *Atp6k* and *Kcr1* showed an inverse correlation. In the PFC, only the transcription of *Tcf21* was common to both strains. In VTA, some of the co-expressed genes exhibited inverse correlations (*Sst*, *Syt5* and *Slc6a4*), whereas *S100a6* and *Tnf* mRNAs were upregulated in both strains.

Consistent with the inherent biological variations between the C3H/HeJ and C57BL/6J strains, nicotine treatment produced substantial differences in gene expression patterns in different brain regions (Tables S1 and S2). Among these, several genes involved in neuronal function and development are noteworthy. For example, glycogen synthase kinase-3 beta

Table 1: Number of genes detected and false discovery rate of each brain region

	C3H/HeJ		C57BL/6J	
Region	Number of significant genes; %*	FDR	Number of significant genes; %	FDR
Amygdala	16↑, 6↓; 3.5	0.10	23↑, 23↓; 7.2	0.18
Hippocampus	16↑, 16↓; 5.0	0.06	39↑, 7↓; 7.4	0.09
NA	69↑, 25↓; 14.7	0.05	68↑, 23↓; 14.3	0.12
PFC	80↑, 31↓; 17.4	0.13	16↑, 14↓; 4.7	0.09
VTA	122↑, 19↓; 22.1	0.07	9↑, 15↓; 4.1	0.07

FDR, false discovery rate.

↑ and ↓, upregulation or downregulation compared with controls.

*The percentages are based on 638 sequence-verified genes on the chips.

(*Gsk3b*) was upregulated by 18% ($P = 0.008$) in the amygdala of C3H/HeJ mice and downregulated by 17% ($P = 0.024$) in the same brain region of the C57BL/6J strain. Potassium channel, subfamily K, member 1 (*Kcnk1*), an inwardly rectifying K^+ channel, was downregulated by 16% ($P = 0.005$) and upregulated by 23% ($P = 0.049$) in the hippocampus of the two strains, respectively. The expression of neuron-specific protein, Purkinje cell protein 19 (PEP-19) (*PCP4*) was downregulated by 33% ($P < 0.001$) and 28% ($P = 0.01$) in the hippocampus of the C3H/HeJ and C57BL/6J mice, respectively.

Table 2: A list of coregulated genes in both C3H/HeJ and C57BL/6J strains within each brain region

			Fold Change	
Region	Gene symbol	Gene name	C3H/HeJ	C57BL/6
Amyg	Protein modification and degradation			
	Usp2	Ubiquitin-specific protease 2	0.83	1.24*
	Signaling transduction			
	Il15	Interleukin 15	1.17	0.79
	Gsk3b	Glycogen synthase kinase- 3 beta	1.18	0.83
	Transport			
	Kcr1	Potassium channel regulator 1	1.20*	0.60
HP	Neuronal structure and transmission			
	Pcp4	Neuron-specific protein PEP-19 (Purkinje cell protein 4)	0.67*	0.72
	Protein modification and degradation			
	Psmb2	Proteasome (prosome, macropain) beta 2 subunit	1.17	1.24
	Protein synthesis			
	Rpl30	Ribosomal protein L30	1.16	1.21
	Transcription factors			
	Tcfeb	Transcription factor EB	1.22	1.18*
	Transport			
	Kcnk1	Potassium channel, subfamily K, member 1	0.84	1.23
NA	Cell division			
	Ask	Activator of S phase kinase	1.16	1.31
	Ccnc	Cyclin C	1.16	1.42*
	Ccng	Cyclin G	1.20	1.33*
	Gspt1	G1 to phase transition 1	1.26	1.65*
	H1f0	H1 histone family, member 0	1.16	1.67*
	Hist4	Histone 4 protein	1.16	1.26
	Cell structure			
	Cugbp2	CUG triplet repeat, RNA-binding protein 2	1.23	1.77*
	Neuronal structure and transmission			
	Hap1	Huntingtin-associated protein	0.80	1.39*
	Nrcam	Neuron-glia-CAM-related cell adhesion molecule	1.23	1.44*
	Signaling transduction			
	Celsr3	Cadherin EGF LAG seven-pass G-type receptor 3	0.82	1.39*
	Dnclc1	Dynein, cytoplasmic, light chain 1	1.19	1.53*
	Fgf2	Fibroblast growth factor 2	1.16	1.40
	Rock1	Rho-associated kinase beta subunit	0.78	1.34
	Transcription factors			
	Pbx3	Pre-B-cell leukemia transcription factor 3	1.19	1.25
	Transport			
	Accn1	Amiloride-sensitive cation channel 1, neuronal (degenerin)	0.73*	1.51
	Atp6k	Vacuolar proton-adenosine triphosphatase subunit M9.2	0.84	1.31
	Kcr1	Potassium channel regulator 1	1.30*	0.68
	Unclassified			
	Mosg	Mosg protein	1.16	1.26
PFC	Transcription factor			
	Tcf21	Transcription factor 21	1.38	1.17

Table 2: *Continued*

Region	Gene symbol	Gene name	Fold Change C3H/HeJ	Fold Change C57BL/6
	Neuronal structure and transmission			
	Chrna4	Nicotinic acetylcholine receptor α 4	1.50*	0.77*
	Grik2	Glutamate receptor, ionotropic, kainate 2	1.24	0.80*
	Signaling transduction			
	Adra1d	Alpha-1A-adrenergic receptor	1.46*	1.15
VTA	S100a6	S100 calcium binding protein A6	1.63	1.26*
	Sst	Somatostatin	1.60*	0.81
	Syt5	Synaptotagmin 5	2.39*	0.78
	Tnf	Tumor necrosis factor, alpha (cachetin)	2.89*	1.17
	Transport			
	Slc6a4	Solute carrier family 6 (neurotransmitter transporter, serotonin), member 4	1.46*	0.78

All genes given in the table are at 0.05 significant level except for those genes marked with *, which indicates a significant level of 0.01.
CAM, cell adhesion molecule; CUG, genetic codon CUG; EGF, epidermal growth factor; LAG, laminin A G-type.

Determination of biological processes associated with nicotine treatment in different brain regions

In addition to determining differentially expressed genes in each brain region of both mouse strains, the overrepresented categories of biological processes within each brain region were analyzed using EASE (Table 3) and representative genes are shown in Tables S5 and S6.

Amygdala

For the C3H/HeJ mice, no overrepresented biological process was detected among either downregulated or upregulated genes, whereas for the C57BL/6J mice, the intracellular signaling cascade process was overrepresented among the upregulated genes (e.g. *Mapk8ip3*, *Map2k1*, *Rab11a* and *Ab11*; Table S5). In addition, the biological process of cell organization/biogenesis was overrepresented among the downregulated genes.

Hippocampus

No overrepresented biological process was detected for the C3H/HeJ strain, while the process related to ubiquitin-dependent protein catabolism, comprising multiple ubiquitin-related genes (e.g. *Uchl5*, *Ube2d2*, *Ubl1* and *Usp5*) and proteasome subunits (e.g. *Psmb2*, *Psmb4*, *Psmb5* and *Psmb6*) was overrepresented in the upregulated genes of C57BL/6J mice (Table S5); and the process related to cellular metabolism and signal transduction were overrepresented in the downregulated genes.

Nucleus accumbens

Although more than 100 significantly regulated genes were detected for this region, only the process of cell cycle/proliferation was overrepresented among the upregulated genes in C3H/HeJ mice (Table S6). Among the four biological processes overrepresented in this region of C57BL/6J mice (Table 3), the categories of cell cycle/proliferation and transmission of nerve impulse were of particular interest. Cell cycle/proliferation was overrepresented in both C3H/HeJ and C57BL/6J mice, and several genes were modulated in both strains (i.e. *Ask*, *Fgf2*, *Ccng*, *Ccnc* and *Gspt1*). For the transmission of nerve impulse category, the genes found to be altered in C57BL/6J mice (e.g. *Gabrd*, *Gria2* and *Grik2*) were different from those for C3H/HeJ mice.

Prefrontal cortex

In contrast to the NA, the cell cycle/proliferation category was downregulated in the PFC of C3H/HeJ mice. Inspection of the list showed several common genes in the PFC and NA (e.g. *Abl1*, *Ccnh*, *Cdc25c* and *Map2k7*). Organogenesis was downregulated, while categories of intracellular signaling cascade and proteolysis/peptidolysis were upregulated in this brain region. For the C57BL/6J mice, transmission of nerve impulses was overrepresented among the upregulated genes, with two genes (*Gria2* and *Mag*) overlapping with the list of the same category in the NA.

Ventral tegmental area

Three biological process categories, i.e. cell-surface receptor-linked signal transduction, intracellular signaling cascade and transmission of nerve impulses, were overrepresented among the upregulated genes in C3H/HeJ mice. For the category of cell-surface receptor-linked signal transduction, most affected genes were part of the integrin-mediated signaling (*Cib1*, *Itga7* and *Itgb7*), G-protein-coupled receptor protein signaling (e.g. *Rgs2*, *Rgs14*, *Gnb2*, *Adra1b* and *Adra1d*), and transmembrane receptor protein tyrosine kinase signaling (*Kdr*, *Egf*, *Ltbp1* and *Bdkrb2*) pathways. For the intracellular signaling cascade, most genes belonged to the protein kinase cascade (e.g. *Mapk13*, *Map4k4*, *Rps6ka2* and *Mapk9*) and small guanosine triphosphatase-mediated signal transduction (*Rheb*, *Rasa3*, *Rhob*, *Arls* and *Rrad*). In the transmission of nerve impulses category, various neurotransmitters were included (Table S6). Interestingly, this category was overrepresented among the downregulated genes of C57BL/6J mice (Table S5).

Table 3: Categories of biological processes overrepresented in each brain region of C3H/HeJ and C57BL/6J

		Downregulated		Upregulated	
Brain region	Biological process category	C3H/HeJ	C57BL/6	C3H/HeJ	C57BL/6
Amyg	Cell organization and biogenesis (29)*	NS	4/23† (0.0766‡)	NS	NS
	Intracellular signaling cascade (60)	NS	NS	NS	6/23 (0.0468)
HP	Ubiquitin-dependent protein catabolism (35)	NS	NS	NS	12/39 (0.0001)
	Cellular metabolism (53)	NS	6/23 (0.0315)	NS	NS
	Cell cycle/proliferation (99)	NS	NS	16/72 (0.1332)	23/69 (0.0002)
NA	Organogenesis (35)	NS	NS	NS	9/69 (0.0277)
	Signal transduction (31)	NS	4/23 (0.0900)	NS	NS
	Transmission of nerve impulse (31)	NS	NS	NS	9/69 (0.0133)
	Vesicle-mediated transport (10)	NS	3/23 (0.0450)	NS	NS
	Cell cycle/proliferation (99)	10/31 (0.0346)	NS	NS	NS
	Intracellular signaling cascade (60)	NS	NS	12/81 (0.1113)	NS
PFC	Ion transport (53)	NS	NS	NS	5/16 (0.0313)
	Organogenesis (35)	5/31 (0.0809)	NS	NS	NS
	Proteolysis and peptidolysis (18)	NS	NS	7/81 (0.0192)	NS
	Transmission of nerve impulse (31)	NS	NS	NS	5/16 (0.0047)
	Cell surface receptor-linked signal transduction (79)	NS	NS	23/126 (0.0473)	NS
VTA	Intracellular signaling cascade (60)	NS	NS	19/126 (0.0324)	NS
	Ion transport (53)	NS	7/18 (0.0017)	NS	NS
	Neurotransmitter transport (4)	NS	2/18 (0.1048)	NS	NS
	Transmission of nerve impulse (31)	NS	6/18 (0.0002)	14/126 (0.0035)	NS

NS, not significant.

*Number in parenthesis under the column of 'Biological process categories' are the number of genes printed on the chips that are belonging to corresponding categories of Gene Ontology: Biological processes.

†Number of downregulated or upregulated genes and the number of regulated genes falling in corresponding biological process categories.

‡EASE score. The categories with EASE score <0.15 are considered as overrepresented.

Determination of unique and common biological processes in C3H/HeJ and C57BL/6J mice

As described earlier, we identified 312 differentially expressed genes in C3H/HeJ and 190 in C57BL/6J mice. PCA using genes as variables allowed for projection of the C3H/HeJ data set (312 variables $\times$ 50 observations) and the C57BL/6J data set (190 $\times$ 50) onto new multidimentional spaces (Fig. 1a,b, respectively). The sudden drop in the eigenvalue contributions with the increasing number of components suggested use of a five-component model for

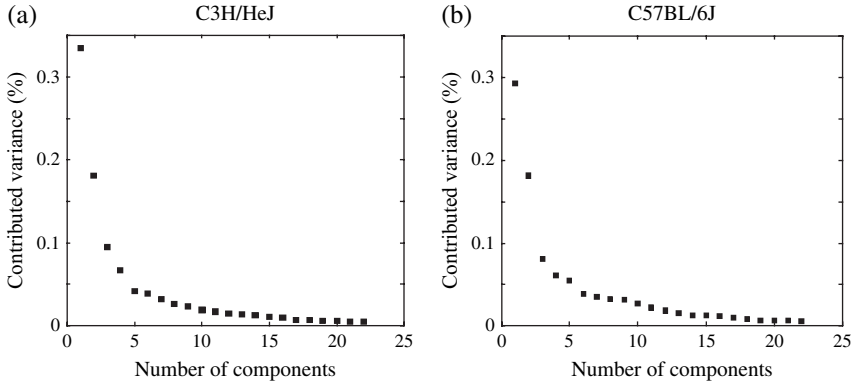

Figure 1: Number of component vs. contributed variance of each component from PCA on differentially expressed genes for the data sets of C3H/HeJ (a) and C57BL/6J (b) mice. For both strains, first 22 components contributing more than 50% of total variance are shown.

both mouse strains, explaining, respectively, 72% and 67% of the total variability observed in the 312 and 190 gene expression data for C3H/HeJ and C57BL/6J mice, respectively. For both mouse strains, 30 genes with the highest absolute loadings were selected for each of the five PCA components. To determine whether the selected 30 genes were involved in certain biological procedures or just randomly distributed, EASE analysis was performed. For C3H/HeJ, cell-surface receptor-linked signal transduction and intracellular signaling cascade biological processes were overrepresented in the first principal component, while cell cycle/cell proliferation, organogenesis, transmission of nerve impulses and cell organization/biogenesis biological processes were overrepresented in the second principal component. No overrepresented category was detected for the remaining three components. For C57BL/6J mice, the biological processes of cell cycle/cell proliferation and organogenesis were overrepresented for the first principal component and the biological processes of transmission of nerve impulses and ubiquitin-dependent protein catabolism for the second and third principal component, respectively. No overrepresented category was detected for the fourth and fifth component. Furthermore, we found that the EASE scores of these categories were stable when 10, 20, 40, 50 and 60 genes with the highest absolute loadings were selected (Fig. 2). This indicates that the biological processes identified here might represent the major contribution in the response to chronic nicotine treatment in the two mouse strains at the whole brain level.

Validation of microarray results by qRT–PCR

The mRNA expression levels of six genes, i.e. *App*, *Apbb2, Aplp2, Homer2*, *Gria2* and *Ikbke*, were validated by qRT–PCR analyses in the PFC region of both strains (Figure S1). These genes were selected because they have been shown to be involved in important biological processes and signaling pathways related to substance abuse (Asztely & Gustafsson 1996; Guenette *et al.* 1996; Kravchenko *et al.* 2003; Soloviev *et al.* 2000) and are regulated by nicotine (Adriani *et al.* 2004; Kane *et al.* 2005; Mochida-Nishimura *et al.* 2001; Tsurutani *et al.* 2005; Wang *et al.* 2007).

For C3H/HeJ animals, microarray analysis showed that two of the six genes were significantly regulated in PFC (*Apbb2*: fold change 1.43, $P = 0.045$; *Ikbke*: fold change 1.36, $P = 0.034$), which were consistent with the result obtained from real-time RT–PCR. Microarray analysis also showed two other genes from the amyloid precursor protein (APP) family were modulated (*APP*: fold change 0.72, $P = 0.056$; *Aplp2*: fold change 1.17, $P = 0.073$), which were also confirmed by the real-time RT–PCR analysis. For genes *Homer2* and *Gria2*, both microarray and real-time RT–PCR analysis showed an insignificant regulation by nicotine in PFC. For C57BL/6J, microarray analysis showed that the expression of four genes, i.e. *APP* (fold change 1.27, $P = 0.013$), *Ikbke* (fold change 1.11, $P = 0.019$), *homer2* (fold change 0.73, $P = 0.042$), *Grai2* (fold change 1.22, $P < 0.001$), were significantly modulated, consistent with the results from real-time RT–PCR. Microarray analysis showed that *Aplp2* (fold change 1.06, $P = 0.463$) and *Apbb2* (fold change 1.15, $P = 0.140$) showed a trend of upregulation although non-significant. Real-time RT–PCR, however, indicated a larger magnitude of upregulation for both genes (*Aplp2*: fold change 1.16, $P = 0.082$; *Apbb2*: fold change 1.78, $P < 0.001$). A comparison of the fold changes of the six genes detected by microarray and real-time RT–PCR showed a correlation coefficient of 0.92 ($P = 0.009$) for C3H/HeJ and 0.82 ($P = 0.046$) for C57BL/6J, further indicating our microarray results were reproducible and reliable.

Discussion

In this study, using cDNA microarrays, we have identified a catalogue of brain region-specific genes that might contribute to the observed strain differences in the physiological

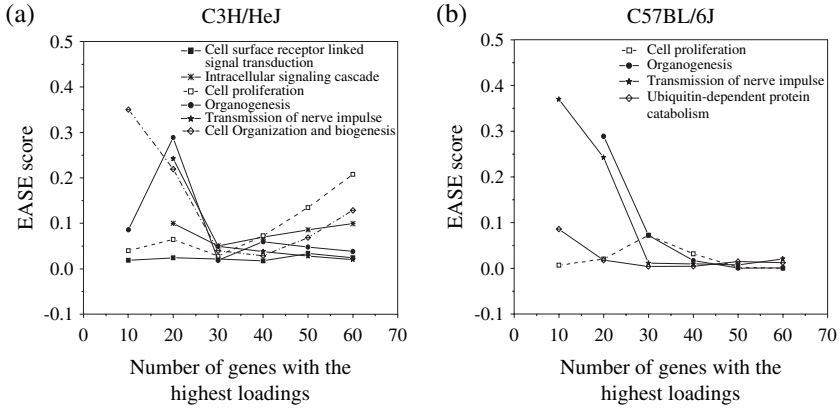

Figure 2: Overrepresented categories of biological processes identified in principal components of PCA. For each strain, the first five principal components were selected, and the 30 genes with the highest absolute loadings were subjected to EASE analysis to detect the overrepresented biological processes. EASE scores at 20, 40, 50 and 60 genes with the highest absolute loadings for each principal component were plotted.

response to chronic oral nicotine treatment. Our study also helped to define significant changes in gene expression patterns that exhibit regional diversity in the brains of C3H/HeJ and C57BL/6J mice in response to nicotine. The number of differentially expressed genes was found to differ substantially between brain regions within and between the two strains (Tables 1, S1 and S2). For instance, PFC and VTA were the two regions in C3H/HeJ mice having the highest number of modulated genes, while the same two regions exhibited relatively fewer transcriptional modulations in C57BL/6J mice. In addition, we found that only a handful of genes were significantly altered in more than two brain regions, suggesting a high degree of brain region specificity in the transcriptional response to nicotine. Comparisons among differentially expressed genes in multiple brain regions also showed that the same set of genes could be modulated inversely in different regions. Together, the complex gene expression architecture identified in this analysis clearly shows the regional diversity and complexity of the brain's response to nicotine.

The biological processes associated with the differentially expressed genes can provide clues to the mechanisms by which each brain region of a specific strain responds to nicotine. Most of the overrepresented biological processes were observed in the NA, PFC and VTA, which play a central role in co-ordinating the rewarding effects of nicotine (Kalivas & Nakamura 1999; Robbins & Everitt 1999). The PCA and EASE analyses were used to show the major biological processes responsible for the variation across brain regions. More categories were identified for C3H/HeJ mice than for C57BL/6J mice, while many categories identified in each strain were overrepresented in at least one brain region. Of the six categories of biological process identified in C3H/HeJ mice, three (i.e. cell cycle/proliferation, organogenesis and transmission of nerve impulses) were also identified in C57BL/6J mice, suggesting that these two strains might exhibit similar functional responses to nicotine treatment.

Nicotine exerts stimulatory or inhibitory effects on the cell cycle and proliferation under different conditions (Chu *et al.* 2005; Hakki *et al.* 2000; Trombino *et al.* 2004). In particular, nicotine increases cell proliferation rates in dividing cells by modulating the Ras-induced expression of cyclin D1 (Chu *et al.* 2005). Modulation of cell cycle-related genes by nicotine in postmitotic neuronal populations is likely to lead to a different cellular response than it produces in mitotic cells (Schmetsdorf *et al.* 2005). Our results indicate that nicotine imposes variable influences on the cell cycle and proliferation in different brain regions. For example, the cell cycle/proliferation process was upregulated in the NA of both C3H/HeJ and C57BL/6J mice, whereas this process was downregulated in the PFC of C3H/HeJ but not of C57BL/6J mice. It is likely that cyclins and associated *cdks* also might have roles other than proliferation in the NA such as neuronal survival and synaptic plasticity. In the PFC of C3H/HeJ mice, the organogenesis category also was downregulated by nicotine. The same regulation patterns of cell cycle/proliferation and organogenesis can be attributed, in part, to the fact that some genes may be involved in both biological processes, although another reason may be that the two processes are coupled and thus change in similar ways.

The process of transmission of nerve impulses includes a series of receptors that are critical to the biological response to nicotine. The transmission of nerve impulses category was overrepresented among the upregulated genes in the VTA of C3H/HeJ mice; but, interestingly, in C57BL/6J mice, it was downregulated in the VTA, while being upregulated in the NA and PFC (Table S6). This finding implies that the mechanism by which the two strains respond to nicotine is different. Nicotine induced upregulation of different cell-surface-based receptors (i.e. *Grik2* and *Syt5*) in the VTA of C3H/HeJ animals, while suppressed the expression of these genes (i.e., *Grik2* and *Syt5*) in this region of C57BL/6J, indicating the differential effects of nicotine treatment on various intracellular signaling pathways in this region. This coordinated differential expression pattern suggests that these two strains, exhibiting highly divergent nicotine-induced behavioral and physiological characteristics, also differ in their nicotine-induced receptor activation, desensitization and inactivation profiles (Laviolette & van der Kooy 2004; Pidoplichko *et al.* 2004).

The expressional profile especially in the VTA region of C3H/HeJ, but not of C57BL/6J, mice was characterized by overrepresentation of genes that belong to the intracellular signaling and signal transduction/receptor categories, particularly to mitogen-activated protein kinase cascade (MAPK) signaling. Previous studies (Konu *et al.* 2004; Nakatani *et al.* 2004) collectively suggest that nicotine exerts its mitogenic and survival-related actions via MAPK. Our findings in this study further support strain-specific MAPK activation by nicotine, as mRNA expression of several genes with essential roles in the production of IP3 and downstream activation of complexes such as PI3K/AKT and others also were upregulated by nicotine in both the PFC and VTA of C3H/HeJ, but not in those of C57BL/6J, mice. These results strongly suggest that the PI pathway-driven MAPK signaling cascade might be relatively more active in C3H/HeJ than in C57BL/6J mice.

Nicotine can alter the expression of various genes involved in multiple signal transduction pathways (Konu *et al.* 2001, 2004; Li *et al.* 2004). The biological process of ubiquitin-dependent protein catabolism was upregulated in the hippocampus of C57BL/6J mice. Although it was not overrepresented in the hippocampus of C3H/HeJ mice, several genes from this pathway were also upregulated (e.g. *Psmb2* and *Uchl1*). The hippocampus is involved in learning and memory, and nicotine can influence the synaptic plasticity in this brain region (Balfour & Ridley 2000; Ji *et al.* 2001). Our results suggest that the physiological influence of nicotine on the hippocampus might be through upregulation of the ubiquitin–proteasome pathway. These findings are consistent with the results of our previous study on nicotine-treated rats (Kane *et al.* 2004) and ethanol-treated cortex neurons (Gutala *et al.* 2004).

It should be noted that, among the genes identified by microarray analysis in the current work, only a limited number of transcripts received independent confirmation using real-time RT–PCR. As pointed previously (Blalock *et al.* 2005; Kane *et al.* 2004; Li *et al.* 2004; Mirnics *et al.* 2001), the major advantage of microarray analysis is not only limited to the identification of single genes, but also its ability to provide a more comprehensive perspective about the regulation of biochemical pathways or functionally related genes. As the current work aimed mainly at detecting the biological

pathways and processes involved in the response to chronic nicotine treatment in the two mouse strains, identifying the overrepresentation of multiple genes related to certain biological pathways or processes not only provides insights regarding the role of the pathways, but also adds confidence to the reliability of the genes identified in the study. However, it is still advisable to take caution when referring to regulation of a specific gene.

In summary, by using a systematic approach to compare the gene expression profiles in five brain regions pertinent to nicotine's actions in C3H/HeJ and C57BL/6J mice, we showed that the expression patterns modulated by nicotine are strain and region specific. In both mouse strains, various biological processes regulated by nicotine were identified. Some of these pathways, e.g. cell cycle/proliferation and transmission of nerve impulses, were commonly regulated in the two strains, indicating that even with the diversity of genes modulated by nicotine, the effects on underlying biological processes appeared similar in certain brain regions. However, we identified several biological process categories with respect to specific signaling pathways (MAPK and ubiquitin–proteasome) whose changes were unique to each mouse strain. It is our hope that this type of approach will help us to understand the interplay between genes and pathways connected to complex behaviors such as nicotine addiction.

References

Adriani, W., Granstrem, O., Macri, S., Izykenova, G., Dambinova, S. & Laviola, G. (2004) Behavioral and neurochemical vulnerability during adolescence in mice: studies with nicotine. *Neuropsychopharmacology* **29**, 869–878.

Asztely, F. & Gustafsson, B. (1996) Ionotropic glutamate receptors. Their possible role in the expression of hippocampal synaptic plasticity. *Mol Neurobiol* **12**, 1–11.

Balfour, D.J. & Ridley, D.L. (2000) The effects of nicotine on neural pathways implicated in depression: a factor in nicotine addiction? *Pharmacol Biochem Behav* **66**, 79–85.

Blalock, E.M., Geddes, J.W., Chen, K.C., Porter, N.M., Markesbery, W.R. & Landfield, P.W. (2004) Incipient Alzheimer's disease: microarray correlation analyses reveal major transcriptional and tumor suppressor responses. *Proc Natl Acad Sci USA* **101**, 2173–2178.

Blalock, E.M., Chen, K.C., Stromberg, A.J., Norris, C.M., Kadish, I., Kraner, S.D., Porter, N.M. & Landfield, P.W. (2005) Harnessing the power of gene microarrays for the study of brain aging and Alzheimer's disease: statistical reliability and functional correlation. *Ageing Res Rev* **4**, 481–512.

Chu, M., Guo, J. & Chen, C.Y. (2005) Long-term exposure to nicotine, via ras pathway, induces cyclin D1 to stimulate G1 cell cycle transition. *J Biol Chem* **280**, 6369–6379.

Crawley, J.N., Belknap, J.K., Collins, A., Crabbe, J.C., Frankel, W., Henderson, N., Hitzemann, R.J., Maxson, S.C., Miner, L.L., Silva, A.J., Wehner, J.M., Wynshaw-Boris, A. & Paylor, R. (1997) Behavioral phenotypes of inbred mouse strains: implications and recommendations for molecular studies. *Psychopharmacology (Berl)* **132**, 107–124.

Crescenzi, M. & Giuliani, A. (2001) The main biological determinants of tumor line taxonomy elucidated by a principal component analysis of microarray data. *FEBS Lett* **507**, 114–118.

Dunckley, T. & Lukas, R.J. (2003) Nicotine modulates the expression of a diverse set of genes in the neuronal SH-SY5Y cell line. *J Biol Chem* **278**, 15633–15640.

Edwards, D. (2003) Non-linear normalization and background correction in one-channel cDNA microarray studies. *Bioinformatics* **19**, 825–833.

Guenette, S.Y., Chen, J., Jondro, P.D. & Tanzi, R.E. (1996) Association of a novel human FE65-like protein with the cytoplasmic domain of the beta-amyloid precursor protein. *Proc Natl Acad Sci USA* **93**, 10832–10837.

Gutala, R., Wang, J., Kadapakkam, S., Hwang, Y., Ticku, M. & Li, M.D. (2004) Microarray analysis of ethanol-treated cortical neurons reveals disruption of genes related to the ubiquitin-proteasome pathway and protein synthesis. *Alcohol Clin Exp Res* **28**, 1779–1788.

Hakki, A., Hallquist, N., Friedman, H. & Pross, S. (2000) Differential impact of nicotine on cellular proliferation and cytokine production by LPS-stimulated murine splenocytes. *Int J Immunopharmacol* **22**, 403–410.

Harlan, R.E. & Garcia, M.M. (1998) Drugs of abuse and immediate-early genes in the forebrain. *Mol Neurobiol* **16**, 221–267.

Hosack, D.A., Dennis, G. Jr, Sherman, B.T., Lane, H.C. & Lempicki, R.A. (2003) Identifying biological themes within lists of genes with EASE. *Genome Biol* **4**, R70.

Ji, D., Lape, R. & Dani, J.A. (2001) Timing and location of nicotinic activity enhances or depresses hippocampal synaptic plasticity. *Neuron* **31**, 131–141.

Kalivas, P.W. & Nakamura, M. (1999) Neural systems for behavioral activation and reward. *Curr Opin Neurobiol* **9**, 223–227.

Kane, J.K., Konu, O., Ma, J.Z. & Li, M.D. (2004) Nicotine coregulates multiple pathways involved in protein modification/degradation in rat brain. *Brain Res Mol Brain Res* **132**, 181–191.

Kane, J.K., Hwang, Y., Konu, O., Loughlin, S.E., Leslie, F.M. & Li, M.D. (2005) Regulation of Homer and group I metabotropic glutamate receptors by nicotine. *Eur J Neurosci* **21**, 1145–1154.

Konu, O., Kane, J.K., Barrett, T., Vawter, M.P., Chang, R., Ma, J.Z., Donovan, D.M., Sharp, B., Becker, K.G. & Li, M.D. (2001) Region–specific transcriptional response to chronic nicotine in rat brain. *Brain Res* **909**, 194–203.

Konu, O., Xu, X., Ma, J.Z., Kane, J., Wang, J., Shi, S.J. & Li, M.D. (2004) Application of a customized pathway-focused microarray for gene expression profiling of cellular homeostasis upon exposure to nicotine in PC12 cells. *Brain Res Mol Brain Res* **121**, 102–113.

Kravchenko, V.V., Mathison, J.C., Schwamborn, K., Mercurio, F. & Ulevitch, R.J. (2003) IKKi/IKKepsilon plays a key role in integrating signals induced by pro-inflammatory stimuli. *J Biol Chem* **278**, 26612–26619.

Laviolette, S.R. & van der Kooy, D. (2004) The neurobiology of nicotine addiction: bridging the gap from molecules to behaviour. *Nat Rev Neurosci* **5**, 55–65.

Li, M.D., Parker, S.L. & Kane, J.K. (2000) Regulation of feeding-associated peptides and receptors by nicotine. *Mol Neurobiol* **22**, 143–165.

Li, M.D., Konu, O., Kane, J.K. & Becker, K.G. (2002) Microarray technology and its application on nicotine research. *Mol Neurobiol* **25**, 265–285.

Li, M.D., Kane, J.K., Wang, J. & Ma, J.Z. (2004) Time-dependent changes in transcriptional profiles within five rat brain regions in response to nicotine treatment. *Brain Res Mol Brain Res* **132**, 168–180.

Marks, M.J., Burch, J.B. & Collins, A.C. (1983) Genetics of nicotine response in four inbred strains of mice. *J Pharmacol Exp Ther* **226**, 291–302.

Marks, M.J., Campbell, S.M., Romm, E. & Collins, A.C. (1991) Genotype influences the development of tolerance to nicotine in the mouse. *J Pharmacol Exp Ther* **259**, 392–402.

Mihailescu, S. & Drucker-Colin, R. (2000) Nicotine, brain nicotinic receptors, and neuropsychiatric disorders. *Arch Med Res* **31**, 131–144.

Mirnics, K., Middleton, F.A., Lewis, D.A. & Levitt, P. (2001) Analysis of complex brain disorders with gene expression microarrays: schizophrenia as a disease of the synapse. *Trends Neurosci* **24**, 479–486.

Mochida-Nishimura, K., Surewicz, K., Cross, J.V., Hejal, R., Templeton, D., Rich, E.A. & Toossi, Z. (2001) Differential activation of MAP kinase signaling pathways and nuclear factor-kappaB in bronchoalveolar cells of smokers and nonsmokers. *Mol Med* **7**, 177–185.

Nakatani, N., Aburatani, H., Nishimura, K., Semba, J. & Yoshikawa, T. (2004) Comprehensive expression analysis of a rat depression model. *Pharmacogenomics J* **4**, 114–126.

Paxinos G. & Franklin K. (2001) *The Mouse Brain in Stereotaxic Coordinates*. Academic Press, San Diego, CA.

Petersen, D.R., Norris, K.J. & Thompson, J.A. (1984) A comparative study of the disposition of nicotine and its metabolites in three inbred strains of mice. *Drug Metab Dispos* **12**, 725–731.

Pich, E.M., Pagliusi, S.R., Tessari, M., Talabot-Ayer, D., Hooft van Huijsduijnen, R. & Chiamulera, C. (1997) Common neural substrates for the addictive properties of nicotine and cocaine. *Science* **275**, 83–86.

Pidoplichko, V.I., Noguchi, J., Areola, O.O., Liang, Y., Peterson, J., Zhang, T. & Dani, J.A. (2004) Nicotinic cholinergic synaptic mechanisms in the ventral tegmental area contribute to nicotine addiction. *Learn Mem* **11**, 60–69.

Pontieri, F.E., Tanda, G., Orzi, F. & Di Chiara, G. (1996) Effects of nicotine on the nucleus accumbens and similarity to those of addictive drugs. *Nature* **382**, 255–257.

Robbins, T.W. & Everitt, B.J. (1999) Drug addiction: bad habits add up. *Nature* **398**, 567–570.

Robinson, S.F., Marks, M.J. & Collins, A.C. (1996) Inbred mouse strains vary in oral self-selection of nicotine. *Psychopharmacology (Berl)* **124**, 332–339.

Schilstrom, B., Fagerquist, M.V., Zhang, X., Hertel, P., Panagis, G., Nomikos, G.G. & Svensson, T.H. (2000) Putative role of presynaptic alpha7* nicotinic receptors in nicotine stimulated increases of extracellular levels of glutamate and aspartate in the ventral tegmental area. *Synapse* **38**, 375–383.

Schmetsdorf, S., Gartner, U. & Arendt, T. (2005) Expression of cell cycle-related proteins in developing and adult mouse hippocampus. *Int J Dev Neurosci* **23**, 101–112.

Soloviev, M.M., Ciruela, F., Chan, W.Y. & McIlhinney, R.A. (2000) Mouse brain and muscle tissues constitutively express high levels of Homer proteins. *Eur J Biochem* **267**, 634–639.

Sparks, J.A. & Pauly, J.R. (1999) Effects of continuous oral nicotine administration on brain nicotinic receptors and responsiveness to nicotine in C57Bl/6 mice. *Psychopharmacology (Berl)* **141**, 145–153.

Trombino, S., Cesario, A., Margaritora, S., Granone, P., Motta, G., Falugi, C. & Russo, P. (2004) Alpha7-nicotinic acetylcholine receptors affect growth regulation of human mesothelioma cells: role of mitogen-activated protein kinase pathway. *Cancer Res* **64**, 135–145.

Tsurutani, J., Castillo, S.S., Brognard, J., Granville, C.A., Zhang, C., Gills, J.J., Sayyah, J. & Dennis P.A. (2005) Tobacco components stimulate Akt-dependent proliferation and NFkappaB-dependent survival in lung cancer cells. *Carcinogenesis* **26**, 1182–1195.

Wang, F., Chen, H., Steketee, J.D. & Sharp, B.M. (2007) Upregulation of ionotropic glutamate receptor subunits within specific mesocorticolimbic regions during chronic nicotine self-administration. *Neuropsychopharmacology* **32**, 103–109.

Winer, J., Jung, C.K., Shackel, I. & Williams, P.M. (1999) Development and validation of real-time quantitative reverse transcriptase-polymerase chain reaction for monitoring gene expression in cardiac myocytes in vitro. *Anal Biochem* **270**, 41–49.

Wonnacott, S., Sidhpura, N. & Balfour, D.J. (2005) Nicotine: from molecular mechanisms to behaviour. *Curr Opin Pharmacol* **5**, 53–59.

Acknowledgment

This project is funded by a grant from the National Institute on Drug Abuse to M.D.L. (DA-13783).

Supplementary material

The following supplementary material is available for this article online from http://www.blackwell-synergy.com/doi/full/10.1111/j.1601-183X.2007.00323.x

Figure S1: Comparison of microarray and quantitative RT–PCR results of six representative genes in the brain region PFC after 14 days of nicotine administration.

Table S1: A list of differentially expressed genes modulated by nicotine in five brain regions for C3H/HeJ strain.

Table S2: A list of differentially expressed genes modulated by nicotine in five brain regions for C57BL/6J strain.

Table S3: Fold change of identified significantly regulated genes by chronic nicotine treatment in two or more brain regions of C3H/HeJ strain.

Table S4: Fold change of identified significantly regulated genes by chronic nicotine treatment in two or more brain regions of C57BL/6J strain.

Table S5: A list of upregulated or downregulated genes included in the overrepresented categories in various brain regions of C57BL/6J strain.

Table S6: A list of upregulated or downregulated genes included in the overrepresented categories in various brain regions of C3H/HeJ strain.

Please note: Blackwell Publishing is not responsible for the content or functionality of any supplementary materials supplied by the authors.